ELASTIC SCATTERING OF 120, 145 AND 172.5 MeV α-PARTICLES BY ^{12}C, ^{24}Mg AND ^{27}Al AND OPTICAL MODEL ANALYSIS

By S. Wiktor*, C. Mayer-Böricke, A. Kiss, M. Rogge, P. Turek

Institut für Kernphysik, Kernforschungsanlage Jülich, D-5170 Jülich, W. Germany

AND

H. Dąbrowski

Institute of Nuclear Physics, Cracow*

(Received November 27, 1980)

The 120, 145 and 172.5 MeV α-particle beams from JULIC were used to measure differential cross sections for elastic scattering on ^{12}C, ^{24}Mg and ^{27}Al in the angular range from about 5° to 70° (c.m. system). The angular distributions were analysed extensively in terms of the optical model using a variety of potential forms. Apart from the parametrized forms of potential, as Woods-Saxon (WS) or rather (WS)^2, also a model independent representation of potential (spline potential) was employed. The analysis based on the parametrized forms of the potential provided the possibility to find best fit parameter sets, which were then examined on their uniqueness and energy dependence. It has been of special interest to gain information on the radial shape of the potential.

PACS numbers: 25.60.–t, 25.60. Cy

1. Introduction

Only a few experiments have been reported so far on α-elastic scattering at incident energies well above 120 MeV. In Ref. [1] α-scattering data are presented for ^{12}C, ^{28}Si, Sn and Pb at 166 MeV. The Maryland group published data for ^{12}C, ^{40}Ca, $^{46,48,50}Ti$, ^{58}Ni, ^{90}Zr and ^{208}Pb at about 140 MeV (Refs. [2–5]). The Jülich-Heidelberg group investigated α-scattering on ^{16}O, ^{12}C, ^{20}Ne and ^{28}Si (Refs. [6, 7]) at energies around 150 MeV and recently the Groningen group (Ref. [8]) has presented a comprehensive study of α-scattering on ^{90}Zr over the energy range from 40 up to 120 MeV.

Elastic scattering data are generally analysed in terms of the optical model. Since the most of reaction theories utilize distorted waves to describe the scattering of the projectile from the target, the extraction of optical potentials from elastic scattering data is the necessary starting point for gaining nuclear structure information from reaction

* Address: Instytut Fizyki Jądrowej, Radzikowskiego 152, 31-342 Kraków, Poland.

processes. Unfortunately, the extraction of optical potential parameters for composite particles suffers at lower incident energies from the well known discrete and continuous ambiguities. It is, however, fairly well established during the past few years [2–4, 9] that unique parameter sets can be obtained for composite particles if the elastic angular distributions are measured at sufficiently high incident α-energy. Such scattering is characterized by the existence of a maximum deflection angle θ_r (rainbow angle), beyond which the differential cross section exhibits an almost exponential fall off. The optical model parameter set providing an overall fit to such an elastic angular distribution, measured well beyond θ_r, does not suffer from discrete ambiguities. It has been also shown (see for example Ref. [2]) that six free parameters appear to be necessary if the classical Woods-Saxon form of potential is used in the analysis of scattering of α-particles at higher incident energies.

This paper presents experimental angular distributions of elastically scattered α-particles on ^{12}C, ^{24}Mg and ^{27}Al at incident energies of 120, 145 and 172.5 MeV and their optical model analysis. The aims of the investigation were: first, to extend the available experimental information for these light nuclei to higher incident energies, next, to provide consistent optical model parameter sets and to study their energy dependence on the basis of data all obtained at the same laboratory. Also the attempts were made to gain information on the radial shape of the potential.

2. Experimental arrangement and results

The experiments have been performed at the Jülich Isochronous Cyclotron JULIC [10] using an energy analysed beam. Beam monitoring was accomplished by means of a Faraday cup located 4 m behind the scattering chamber and additionally by a monitor detector. The beam was focussed on the target to a spot of less than 2 mm diameter. The targets used in the experiments were self supporting foils of natural ^{12}C and ^{27}Al and highly enriched ^{24}Mg, with thicknesses around 3 mg/cm^2. The zero point of the absolute angular scale was determined to be better than 0.03°. This was estimated by the energy calibration of the two peaks of α-particles scattered on hydrogen in a $(CH)_x$ target.

The target and the detector telescopes were placed inside a 1 m diameter scattering chamber. The scattered particles were detected and identified by the detector telescopes operating in the usual ΔE-E mode. The ΔE detectors were Si surface-barrier counters while the E detectors were Ge(Li) diodes of the side entry type [11] produced in the detector laboratory of the Institute. The energy resolution in the particle spectra was about 150 keV. This was sufficient to separate the elastic peak from the first inelastic peak in all spectra.

Spectra were obtained for ^{24}Mg at 145 and 172.5 MeV and for ^{12}C and ^{27}Al at 120, 145 and 172.5 MeV incident α-energies from about 5° to 70° (c.m.). The experimental angular distributions resulting from these measurements are shown in Fig. 1 (points). They show a diffraction pattern at small angles and a rapid fall off with weak structure at larger angles which supports the conjecture of rainbow scattering [4].

The main uncertainties in the evaluation of the cross sections were those due to target thickness, beam current integration and solid angles. The error in the absolute cross

section (common normalization error) is estimated to be less than 15% for all three nuclei. The relative error is smaller than 10%. Except for the data points at the largest angles, the errors resulting from counting rate are smaller than the data points in Fig. 1.

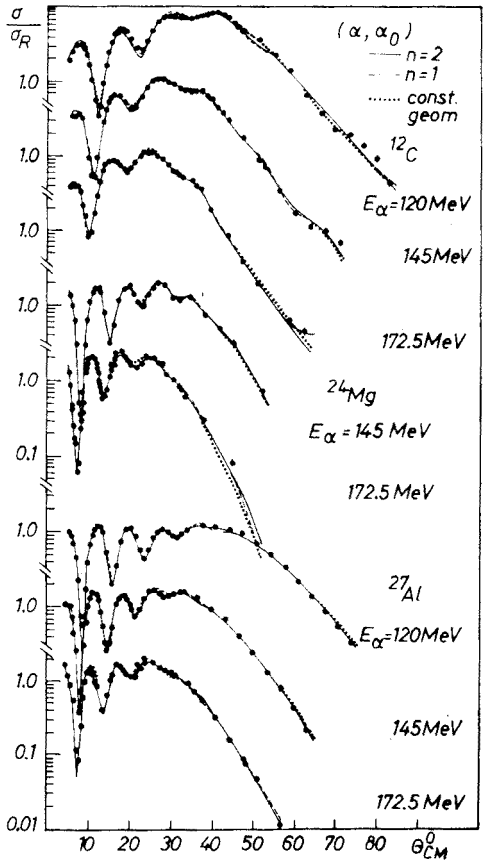

Fig. 1. Elastic α-scattering cross section normalized to the Rutherford cross section. Solid lines represent the 6-parameter $(WS)^2$ fits, dashed lines represent the 6-parameter WS fits and dotted lines represent the 2-parameter WS fits with constant geometry

3. Optical Model analysis with the Woods-Saxon potential

We began the analysis of the data using the standard Woods-Saxon (WS) form of potential [12] with either volume absorption

$$U(r) = V_C(r, r_C) - V \cdot f(r, r_V, a_V) - i \cdot W_V \cdot f(r, r_{WV}, a_{WV}) \tag{1}$$

or surface absorption

$$U(r) = V_C(r, r_C) - Vf(r, r_V, a_V) + i4a_{WS}W_S \frac{d}{dr} f(r, r_{WS}, a_{WS}), \tag{2}$$

where $f(r, r_i, a_i) = (1+\exp[(r-r_iA^{1/3})/a_i])^{-1}$ and $V_C(r, r_C)$ is the Coulomb potential of a uniformly charged sphere of radius $r_C \cdot A^{1/3}$. In accordance with Refs. [1, 4] a value of 1.3 fm for the Coulomb radius r_C was used throughout these analyses.

In order to find the best optical model parameter sets the quantity

$$\chi^2 = \frac{1}{N}\sum_{i=1}^{N}\left[\frac{\sigma(\theta_i)-\sigma_{exp}(\theta_i)}{\Delta\sigma_{exp}(\theta_i)}\right]^2$$

was minimized with $\sigma(\theta_i)$ being the Optical Model differential cross sections and $\sigma_{exp}(\theta_i)$ and $\Delta\sigma_{exp}(\theta_i)$ denoting the experimental cross sections and errors at angles θ_i, respectively. The calculations were performed by using Raynal's computer program MAGALI [12].

At the beginning of the analysis we have tested the uniqueness of the potential parameters and verified whether the volume absorption produces better fits than the surface absorption. For these purposes, a V-grid search was performed by fixing V at a number of different values in the range from about 80 to 190 MeV. The remaining five parameters

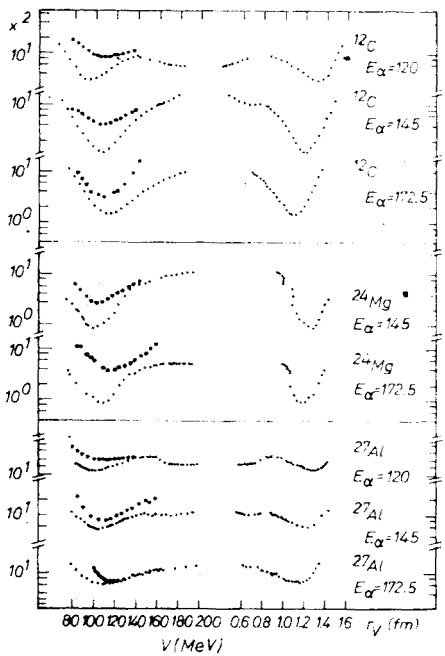

Fig. 2. The minimized values of χ^2 vs. V (left side) and χ^2 vs. r_V (right side) for volume absorption (crosses) and surface absorption (dots) using a WS type potential

(r_V, a_V, W, r_W, a_W) were allowed to vary in order to minimize χ^2. Several such V-grid searches were performed using different starting parameter sets, including also the additional case of a fixed r_V to make sure that no discrete potential family was missed. This procedure has been employed in the analysis of all experimental data for both volume and surface

type absorption. The results are presented in Fig. 2. On the left side the minimized values of χ^2 are plotted versus V. It is seen that for ^{12}C and ^{24}Mg volume absorption (crosses) gives definitely better agreement with experimental data than surface absorption (points). This applies also for ^{27}Al in the cases of 120 and 145 MeV. At 172.5 MeV this feature is not so obvious. However, the visual quality of the fits tends to prefer volume absorption also in this latter case. On the basis of these results, only volume absorption is considered later in the discussions. This result agrees with α-scattering analyses done at lower incident energies [2–4]. The corresponding plots for χ^2 vs. r_V in the case of volume absorption are shown on the right side in Fig. 2.

Simultaneously we answered the question of the discrete potential ambiguities for the case of our data. If such ambiguities were present in the large V range investigated, they should show up in the χ^2 vs. V plots of Fig. 2 as additional minima as deep as the main minimum, [9]. Since no such effect is apparent, we conclude that the potentials found for the χ^2 minima are unique for our high incident energies. Similarly, as it has been practiced in Refs. [4] and [9] test searches have been performed in order to demonstrate that the large angle data play a critical role in removing the discrete ambiguities. For these tests the experimental data sets were gradually truncated from the side of large angles. If the data were truncated at angles below 30° a new discrete family of parameters originated, which equally well fitted the data.

TABLE I

Optimum WS parameter sets (volume absorption) corresponding to the minima in the χ^2 plots of Fig. 2

Target	E_α (MeV)	V (MeV)	r_V (fm)	a_V (fm)	W (MeV)	r_W (fm)	a_W (fm)	χ^2	rms-radius (fm)	$J/4A$ (MeV · fm^3)
^{12}C	120	97.9	1.340	0.74	17.3	1.856	0.47	3.08	3.635	388.
	145	111.2	1.200	0.80	15.8	1.883	0.50	1.25	3.656	370.
	172.5	112.8	1.140	0.82	16.8	1.822	0.53	1.47	3.657	346.
^{24}Mg	145	100.8	1.282	0.78	20.4	1.745	0.48	3.52	4.075	325.
	172.5	111.0	1.178	0.85	23.4	1.626	0.62	3.48	4.112	308.
^{27}Al	120	101.4	1.318	0.74	20.2	1.679	0.56	12.5	4.117	328.
	145	107.1	1.230	0.79	19.7	1.632	0.62	5.44	4.098	304.
	172.5	109.8	1.163	0.81	21.7	1.548	0.70	5.98	4.047	278.

The optimum parameter sets corresponding to the χ^2 minima of Fig. 2 are summarized in Table I. In this Table there are also listed the root mean square (rms) radii of interaction evaluated for these parameters according to the formula commonly used [13] in the case of a WS formfactor.

The differential cross sections, calculated from these potentials are displayed in Fig. 1. With respect to the parameters in Table I, we want to emphasize that a large difference between the parameters r_V and r_W is noticed in all cases, r_W being much larger than r_V. This feature is in accordance with the results of Refs. [1–4, 6, 7] and [9]. It seems therefore to be a general feature of α-scattering.

In order to examine the question of continuous ambiguities in the optical model parameters, the volume integrals $J/4A$ (per projectile-target nucleon pair) have been evaluated using the formula given in Ref. [14]. Their numerical values, corresponding to optimum fit parameters, are given in Table I. As expected for a definite potential family, obtained from lower incident energy data [14], the volume integrals were found to be approximately constant within some range of V, and especially in the neighbourhood of the narrow minimum of χ^2 versus r_V (Fig. 2). Outside these limits of constancy, the $J/4A$ value changes sharply. This V-range, together with the corresponding range of fluctuations of $J/4A$ values, is given in Table II for the nuclei and energies studied.

TABLE II

Ranges of fluctuations of volume integrals $J/4A$ (under the requirement that they are approximately constant) and corresponding V parameter ranges for WS type analysis

Target	E_α (MeV)	V-range (MeV)	$J/4A$-range MeV · fm^3
^{12}C	120	80–106	382–392
	145	85–147	362–372
	172.5	100–175	340–350
^{24}Mg	145.	81–152	310–325
	172.5	84–126	302–318
^{27}Al	120	84–117	312–328
	145	79–114	300–318
	172.5	84–131	266–278

Table I shows that the integral quantities such as the rms radii and the volume integrals behave under the change of energy as expected from the model, i.e. the rms radii remain almost constant and the volume integrals decrease systematically with increasing incident energy. Slopes of -0.95 MeV · fm^3/MeV and -0.84 MeV · fm^3/MeV of volume integrals are found for ^{27}Al and ^{12}C, respectively. A variation of the normalization of the cross section of about 20% is reflected in a 5% change in the values of the volume integral. Smith et al. [2] report a slope of -1.1 MeV · fm^3/MeV for ^{12}C using their own 139 MeV data and additional data taken by other groups at 104 and 166 MeV. In medium weight nuclei the slope of the volume integral is about 0.3–0.6 MeV · fm^3/MeV [8, 15, 16]. Furthermore, at constant incident energy the volume integrals for ^{12}C, ^{24}Mg and ^{27}Al scattering decrease considerably with increasing mass number (Table I). However, if the present results at 145 MeV and those of Ref. [4] around 140 MeV are combined, no monotonic variation of the value of the volume integral with A can be established, in contrast to the suggestion in Ref. [4]. This can be seen from the $J/4A$ values for ^{24}Mg (E_α = 145 MeV) and ^{27}Al (E_α = 145 MeV), which are already smaller than that for ^{40}Ca (E_α = 142 MeV), in Ref. [4]. This anomaly may be understood by taking into account that in contrast to the nuclei studied by Goldberg et al. [4] the ^{24}Mg and ^{27}Al nuclei are deformed. Therefore,

it may be worthwhile to perform experiments on heavier target nuclei and to do coupled channel calculations in order to find out whether the parameters describing the elastic scattering within this framework would exhibit a smoother A-dependence of the volume integral. Such problems have been previously discussed in the case of α-scattering in the rare-earth region [17].

The existence of continuous ambiguities between the parameters of the potential makes it impossible to examine the energy dependence of individual parameters of the potential reliably. For instance, from our analysis has emerged the increase of the parameter V and the decrease of the parameter r_V, when the energy increases (Table I). Such increase of V is of course unphysical and indicates inadequate potential form. In Sections 4 and 5 we consider therefore other potential forms.

In case of the WS potential we have performed additional analyses of the data, as it is often practiced by authors, who examine the subject of energy dependence of the potential [8, 18, 19], by fixing the geometrical parameters. In the first step only the parameter r_V was fixed; the value of $r_V = 1.20$ fm for ^{12}C and $r_V = 1.23$ fm for ^{27}Al, i.e. those being optimal for $E_\alpha = 145$ MeV, have been used. This approach resulted immediately in producing a decrease of the parameter V with increasing energy, however, the fits became markedly worse (in χ^2) than the six parameter fits. Upon fixing, in a similar way, the remaining geometrical parameters the real potential depth decreased almost linearly with increasing energy of incident α-particles, but the χ^2-values became still worse. Similar deterioration of fits, when fixing the geometry, have been observed also in other cases [8, 19–21].

4. Modification of the WS form of potential

For many years the WS potential form was commonly used as capable of giving satisfactory reproduction of scattering data. Microscopic calculations, however, which were performed in the last few years [8, 22–26] indicated that the true form of the potential, especially in the surface and tail region, differs from that of the WS type. The model independent representations in terms of spline functions [8, 27], or the Fourier-Bessel expansion of the potential [28] have recently proved that a modification of the WS form of potential is necessary.

To account to some extent for the modification of the potential form some authors have attempted to use the square [8, 15, 16, 19, 26] or other adjustable power [30, 31] of the WS form. In this chapter a systematic study of the optimum power of the WS form will be presented [32]. We examined a parametrized form of potential

$$V(r) = V_C(r, r_C) - V \cdot f(r, r_V, a_V)^n - iW \cdot f(r, r_W, a_W)^m \tag{3}$$

where n and m are adjustable powers and the other symbols have the same meaning as in formula (1). Our method differs slightly from that of Michel et al. [30] by allowing different geometrical parameters in the real and imaginary parts and by changing the powers n and m independently.

The analysis was started with $n = m$. The value of n was fixed to a series of values between 0.8 and 3.0 and all six parameters of the potential were allowed to vary until

the lowest value of χ^2 was reached for a given n. This approach has shown that an increase of n is accompanied by an increase of all potential parameters. This can be easily explained since the rise of the power of the WS form makes this form of potential more shallow in the surface region. This region, however, is mostly probed in the scattering of α-particles, hence, the requirement to fit the data with a shallower potential requires in turn the strength and the radii of the potential to be respectively larger. It appears that the potential parameters and the magnitudes of n are strongly correlated, thus giving rise to a new ambiguity.

The variation of χ^2 with n is displayed for different nuclei and different energies in Fig. 3. Full lines correspond to $n = m$, i.e. to the same shapes of the real and imaginary part. The resulting χ^2 values correspond in every point to the set of parameters producing

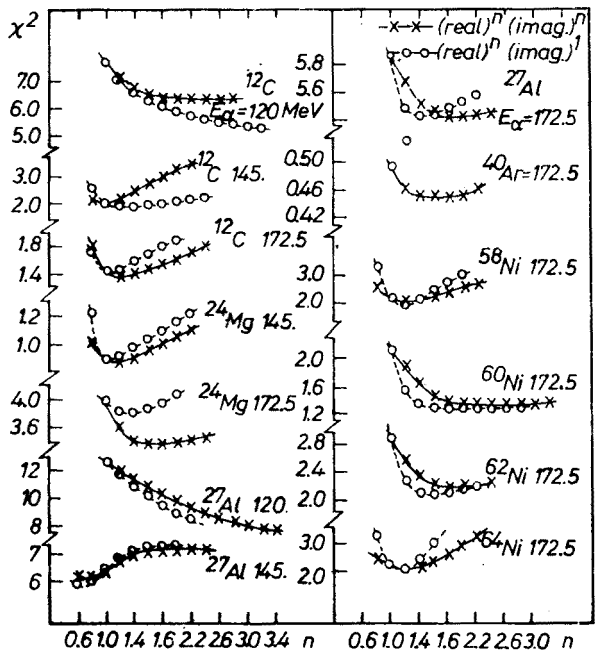

Fig. 3. The dependence of χ^2 on the power n. Solid lines correspond to $n = m$ and dashed lines correspond to m constant ($m = 1$). The data for ^{40}Ar and $^{58-64}$Ni were taken from Refs. [33] and [34] respectively

optimum fits to the experimental data. From this figure it is seen that in the majority of cases one gets an improvement of the fits if the value of n is chosen greater than one. In the case of the lowest energies, i.e. of 120 MeV for ^{12}C and ^{27}Al the values of n tend to increase monotonically with decreasing χ^2; however, the strength of the potential increases beyond reasonable limits. Moreover, it looks from Fig. 3 as if the optimum power n and hence the radial form of the potential changed, when the target nuclei and the beam energy were changed. Obviously a standard, optimum n for different targets and different energies can not be found. On the basis of these results one can not claim that the square of the WS form is more suitable than the WS form.

The solid lines in Fig. 1 correspond to the fits with $n = 2$. Except for the largest angles, the differences between the fits, corresponding to WS and $(WS)^2$ forms, are negligible. The unphysical energy dependence of V (Section 3) remains resistant to the change of the WS into the $(WS)^2$ form of the potential.

To examine the problem, whether the forms of the real and imaginary parts of the potential are the same, the analysis based on formula (3) was continued varying only the value of n and keeping constant the value of m. The dashed lines in Fig. 3 correspond to the case of $m = 1$. Since in some cases the dashed lines are below the full lines one can conclude from Fig. 3 that from the point of view of the data analysis different forms of the real and imaginary parts are allowed and that each of them could vary independently with energy. Different forms of the real and imaginary part of the potential were considered also in some microscopic calculations [23–26].

The question arises how the curves, displayed in Fig. 3, are changed by experimental errors. This problem was examined by means of introducing artificially a systematic and relative error into the experimental data. The systematic error was simulated by changing the normalization of experimental data, and the relative error was introduced by changing a little the error of the data for some angles. Fig. 4 illustrates the effect of the change

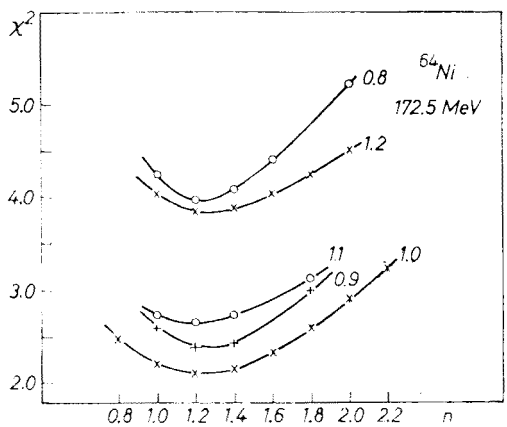

Fig. 4. The dependence of χ^2 on the power n in the case of ^{64}Ni. Various curves correspond to various normalizations

of normalization. As it is seen from this figure, the shape of the curves and the positions of the minima are practically unaffected by the change of systematic error. The relative error, however, influences seriously, as has been proved, the shapes and positions of minima of the curves presented on Fig. 3. Especially careful estimation of this error is needed at the points where the cross section changes rapidly with angle and at the large angles where the statistics is poor and the background is large. In view of these facts the conclusions, drawn from Fig. 3, must be taken only as tentative and not much importance should be attached to them.

5. *Model independent analysis (spline function method)*

In order to avoid the constraints imposed by the parametrized form of the potential a model independent analysis of the scattering data has been performed. Among the other possibilities [28, 35] we chose the spline function method [8, 27] as having a large "elasticity" to accommodate the radial form of potential for structural effects and being capable to account for possible fluctuations in the potential strength and potential form with the change of incident energy. Similarly as in Refs. [8] and [27] we represented the real part of the potential by 11 discrete values $V(r_i)$ ($i = 0, 1 \ldots 10$) between 0 and 10 fm; the imaginary part $W(r)$ was represented by a WS form. In summary 14 parameters were searched simultaneously to achieve a minimum in the χ^2 value. The program OPTY [36] accomplished the interpolation of the potential between the specific radii by a smoothly varying function constructed from cubic polynomials. For calculation of the error band we prepared a special code OPTER. The extension of the error band is determined from mutual correlations between the parameters within the range imposed by the criterion $\chi^2 = \chi^2_{\min} + 1$. The estimated experimental errors are of great importance in gaining a true form of the potential and reasonable extension of the error band.

The model independent analysis generally resulted in considerably better fits than obtained in the analysis based on WS or $(WS)^2$ forms of the potential (Table III). In Fig.

TABLE III

The rms radii of interaction, the volume integrals and χ^2-values resulting from the spline function calculations

Target	E_α (MeV)	rms-radius (fm)	$J/4A$ (MeV · fm^3)	χ^2
^{12}C	120	3.615 ± 0.099	346.8 ± 12.0	1.90
	145	3.620 0.061	376.1 8.3	0.66
	172.5	3.550 0.125	330.3 12.1	1.08
^{24}Mg	145	4.030 0.072	321.0 6.8	0.77
	172.5	4.118 0.099	310.2 13.0	1.82
^{27}Al	120	3.868 0.053	298.4 9.34	3.72
	145	4.089 0.130	299.9 10.9	3.35
	172.5	3.927 0.128	270.9 10.2	3.49

5 there are illustrated the radial shapes of potential $V(r)$ found by the spline analysis. Shaded lines in this figure represent the limits of the error band and dashed lines correspond to the WS form of $V(r)$ calculated from the best fit parameters, given in Table I. It can be seen from this figure that the spline formfactor (full lines) and the WS formfactor (dashed lines) practically overlap in the radial range of 3–7 fm ("sensitivity region"). In this range of radii the error band is narrow; it becomes broad outside this range, where also appreciable deviations between the spline formfactor and the WS formfactor show up.

In Table III there are listed the integral quantities as the rms radii of interaction and the volume integrals. It is seen from Tables I and III that the difference in rms radii, determined by both methods, does not exceed 6%. The rms radii obtained from the WS form-factor are almost constant when the energy is varied, whereas those obtained from the spline method, exhibit uncorrelated variations with energy. This is evidently due to the poor determination of $V(r)$ by the spline method in the centre and the tail region. Accor-

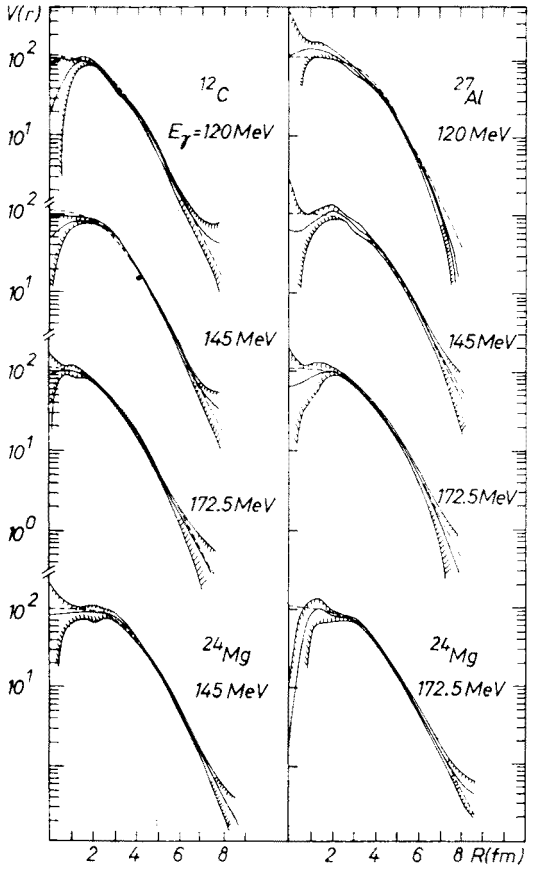

Fig. 5. The radial shapes of the potential $V(r)$ found by the spline analysis. Shaded lines denote the limits of the error band and the dashed lines correspond to the WS form of $V(r)$ calculated from the best fit parameters

dingly, the volume integrals show a similarly irregular behaviour, determined by the use of the spline function method.

Looking at Fig. 5 one can understand, that by the use of the parametrized form of the potential as WS or $(WS)^v$ we can always obtain good fits, because the radial form of the potential in the sensitivity region can always be adjusted to resemble the shape of the potential, found by the spline method.

6. Conclusions

This work demonstrates the absence of discrete ambiguities in the real WS potential depth, when the energy of the bombarding particles increases in the elastic scattering of α-particles on ^{12}C, ^{27}Al and ^{24}Mg; it was shown in addition how the continuous ambiguity in this potential can be restricted. Further, it was demonstrated, that the volume absorption is superior to the surface absorption in α-scattering at relatively high incident energy for the light nuclei investigated.

The analysis of elastic scattering in terms of an optical potential with the WS form has given satisfactory fits providing that six parameters are searched. The average quantities, as rms radii and volume integrals, evaluated by use of optimum fit parameters, behave consistently with the change of incident energy i.e. the rms radii remain approximately constant and the volume integrals decrease roughly linearly with increasing energy.

The model independent form of the potential in terms of the spline functions allowed to describe successfully the angular distributions of scattered α-particles. It has been shown, that in the range of 3–7 fm the parametrized potential lies generally inside the narrow error band of the spline potential. Modifications of the WS form of potential have also been investigated. It seems to be of interest to gain more information on the question of equality of the real and imaginary formfactors as well as on possible mass and energy dependence of these formfactors; however, information on such details is especially sensitive to the accuracy of the data.

We thank Professor A. Budzanowski and Professor D. A. Goldberg for helpful discussions.

REFERENCES

[1] B. Tatischeff, I. Brissaud, *Nucl. Phys.* **A155**, 89 (1970).
[2] S. M. Smith, G. Tibell, A. A. Cowley, D. A. Goldberg, H. G. Pugh, W. Reichart, N. S. Wall, *Nucl. Phys.* **A207**, 273 (1973).
[3] D. A. Goldberg, S. M. Smith, G. H. Pugh, P. G. Roos, N. S. Wall, *Phys. Rev.* **C7**, 1938 (1973).
[4] D. A. Goldberg, S. M. Smith, C. F. Burdzik, *Phys. Rev.* **C10**, 1362 (1974).
[5] P. L. Robertson, D. A. Goldberg, N. S. Wall, L. W. Woo, H. L. Chen, *Phys. Rev. Lett.* **42**, 54 (1979).
[6] K. T. Knöpfle, G. J. Wagner, H. Breuer, M. Rogge, C. Mayer-Böricke, *Phys. Rev. Lett.* **35**, 779 (1975).
[7] K. T. Knöpfle, G. J. Wagner, A. Kiss, M. Rogge, C. Mayer-Böricke, Th. Bauer, *Phys. Lett.* **64B**, 263 (1976).
[8] L. W. Put, A. M. J. Paans, *Nucl. Phys.* **A291**, 93 (1977).
[9] D. A. Goldberg, S. M. Smith, *Phys. Rev. Lett.* **29**, 500 (1972).
[10] C. Mayer-Böricke, Report of the Kernforschungsanlage Jülich, West Germany, JÜL-665-KP (1970).
[11] G. Riepe, D. Protić, *Nucl. Instrum. Methods* **101**, 77 (1972); G. Riepe, D. Protić, J. Reich, *Nucl. Instrum. Methods* **124**, 527 (1975); G. Riepe, D. Protić, *IEEE Trans. Nucl. Sci.* NS-22, 1 (1975).
[12] J. Raynal, *Optical Model Program MAGALI*, CEN Saclay, Boite Postale No. 2, 92 Gif-Sur-Yvette, France.
[13] G. W. Greenlees, G. J. Pyle, Y. C. Tang, *Phys. Rev.* **171**, 1115 (1968).

[14] D. C. Weisser, J. S. Lilley, R. K. Hobbie, G. W. Greenless, *Phys. Rev.* **C2**, 544 (1970).
[15] A. Budzanowski, H. Dabrowski, L. Freindl, K. Grotowski, S. Micek, R. Planeta, A. Strzałkowski, M. Bosman, P. Leleux, P. Macq, J. P. Meulders, C. Pirart, *Phys. Rev.* **C17**, 951 (1978).
[16] Th. Delbar, Gh. Gregoire, G. Paić, R. Ceuleneer, G. Michel, R. Vanderpoorten, A. Strzalkowski, A. Budzanowski, H. Dabrowski, L. Freindl, K. Grotowski, S. Micek, R. Planeta, *Phys. Rev.* **C18**, 1237 (1978).
[17] N. K. Glendenning, D. L. Hendrie, O. N. Jarvis, *Phys. Lett.* **26B**, 131 (1968).
[18] D. F. Jackson, R. C. Johnson, *Phys. Lett.* **49B**, 249 (1974).
[19] H. H. Chang, B. W. Ridley, T. H. Braid, T. W. Conlon, E. F. Gibson, N. S. P. King, *Nucl. Phys.* **A270**, 413 (1976).
[20] H. Eickhoff, D. Frekers, H. Löhner, K. Poppensieker, R. Santo, G. Gaul, C. Mayer-Böricke, P. Turek, *Nucl. Phys.* **A252**, 333 (1975).
[21] L. W. Put, A. M. J. Paans, *Phys. Lett.* **B49**, 266 (1974).
[22] A. Budzanowski, A. Dudek, K. Grotowski, A. Strzalkowski, *Phys. Lett.* **32B**, 431 (1970).
[23] Z. Majka, A. Budzanowski, K. Grotowski, A. Strzalkowski, *Phys. Rev.* **C18**, 114 (1978).
[24] N. Vinh Mau, *Phys. Lett.* **71B**, 5 (1977).
[25] A. Budzanowski, A. Dudek, K. Grotowski, Z. Majka, A. Strzalkowski, *Part. Nucl.* **6**, 97 (1974).
[26] F. A. Brieva, J. R. Rook, *Nucl. Phys.* **A291**, 299, 317 (1977).
[27] F. Michel, R. Vanderpoorten, *Phys. Lett.* **82B**, 183 (1979).
[28] E. Friedman, C. J. Batty, *Phys. Rev.* **C17**, 34 (1978).
[29] D. A. Goldberg, *Phys. Lett.* **55B**, 59 (1975).
[30] F. Michel, R. Vanderpoorten, *Phys. Rev.* **C16**, 142 (1977).
[31] H. P. Gubler, U. Kiebele, H. O. Meyer, G. R. Plattner, I. Sick, *Phys. Lett.* **B74**, 202 (1978).
[32] S. Wiktor, C. Mayer-Böricke, A. Kiss, M. Rogge, P. Turek, *Lecture Notes in Physics*, edited by J. Ehlers et al.; 89; Springer-Verlag Berlin, Heidelberg, New York 1979, p. 315.
[33] A. Budzanowski, C. Alderliesten, J. Bojowald, C. Mayer-Böricke, W. Oelert, P. Turek, S. Wiktor, KFA Annual Report 1977, p. 1.
[34] J. P. Didelez, C. Mayer-Böricke, W. Oelert, M. Rogge, P. Turek, S. Wiktor, *Nucl. Phys.* **A318**, 205 (1979).
[35] N. S. Wall, A. A. Cowley, R. C. Johnson, A. M. Kobos, *Phys. Rev.* **C17**, 1315 (1975).
[36] H. Dabrowski, R. Planeta, A. Djaloeis, Jül-1637 (1980).